Journal of Saudi Chemical Society (2023) 27, 101613

King Saud University

Journal of Saudi Chemical Society

www.ksu.edu.sa
www.sciencedirect.com

ORIGINAL ARTICLE

# Evaluation of the effects of the presence of ZnO - $TiO_2$ (50 %–50 %) on the thermal conductivity of Ethylene Glycol base fluid and its estimation using Artificial Neural Network for industrial and commercial applications

**As'ad Alizadeh [a], Khidhair Jasim Mohammed [b], Ghassan Fadhil Smaisim [c,d], Salema K. Hadrawi [e,f], Hussein Zekri [g,h], Hamid Taheri Andani [i], Navid Nasajpour-Esfahani [k], Davood Toghraie [j,*]**

[a] *Department of Civil Engineering, College of Engineering, Cihan University-Erbil, Erbil, Iraq*
[b] *Air Conditioning and Refrigeration Techniques Engineering Department, Al-Mustaqbal University College, Babylon. Iraq*
[c] *Department of Mechanical Engineering, Faculty of Engineering, University of Kufa, Iraq*
[d] *Nanotechnology and Advanced Materials Research Unit (NAMRU), Faculty of Engineering, University of Kufa, Iraq*
[e] *Refrigeration and Air-conditioning Technical Engineering Department, College of Technical Engineering, The Islamic University, Najaf, Iraq*
[f] *Computer Engineering Department, Imam Reza University, Mashhad, Iran*
[g] *College of Engineering, The American University of Kurdistan, Duhok, Kurdistan Region, Iraq*
[h] *Department of Mechanical Engineering, College of Engineering, University of Zakho, Zakho, Kurdistan Region, Iraq*
[i] *Department of Electronic Engineering, Isfahan University of Technology, Isfahan, Iran*
[j] *Department of Mechanical Engineering, Khomeinishahr Branch, Islamic Azad University, Khomeinishahr, Iran*
[k] *Department of Material Science and Engineering, Georgia Institute of Technology, Atlanta 30332, USA*

Received 2 February 2022; revised 27 December 2022; accepted 22 January 2023
Available online 26 January 2023

**KEYWORDS**

ZnO;
$TiO_2$;

**Abstract** In this study, the thermal conductivity ($k_{nf}$) of ZnO -$TiO_2$ (50 %–50 %)/ Ethylene Glycol hybrid nanofluid using Artificial Neural Networks (ANNs) was predicted. The nanofluid was prepared at different volume fractions ($\varphi$) of nanoparticles ($\varphi$ = 0.001 to 0.035) and temperatures

* Corresponding author.
E-mail address: Toghraee@iaukhsh.ac.ir (D. Toghraie).
Peer review under responsibility of King Saud University. Production and hosting by Elsevier.

Production and hosting by Elsevier

https://doi.org/10.1016/j.jscs.2023.101613

Nanofluid;
Thermal conductivity;
Artificial Neural Networks

(T = 25 to 50 °C). In this study, an algorithm is presented to find the best neuron number in the hidden layer. Also, a surface fitting method has been applied to predict the $k_{nf}$ of nanofluid. Finally, the correlation coefficients, performances, and Maximum Absolute Error (MAE) for both methods have been presented and compared. It could be understood that the ANN method had a better ability in predicting the $k_{nf}$ of nanofluid compared to the fitting method. This method not only showed better performance but also reached a better MAE and correlation coefficient.



## 1. Introduction

Nanofluids have emerged as a new approach in the field of thermal engineering. Nanofluids consist of a suspension of solid nanoparticles or fibers less than 100 nm in a base fluid. The good dispersion of solid particles in a liquid is commonly known as a colloidal suspension. The study of heat transfer in solids dispersed in liquids has been carried out in recent years. The main obstacle to using microparticles is increased corrosion and abrasion in engineering systems. With the advent of nanotechnology, the use of nanoparticles led to the creation of a stable colloidal system, later known as nanofluids. Unlike micro-sized suspensions, nanoparticles can form a high-strength system used in systems where a fluid is used to transfer energy. Today, most equation optimizations are performed using ANNs, as this method optimizes your outputs with great accuracy, and you can then enter into other studies such as simulation. Optimization is, of course, an ANN feature. In recent years, ANNs have found many applications in various engineering sciences. The use of ANNs in different branches of engineering is increasing day by day and covers different ranges, so engineers must know how it works and how to use it [1,2]. Kumar et al. [3] predicted the $k_{nf}$ of Cu-Zn/ $H_2O$ hybrid Newtonian nanofluids using ANNs and experimental methods. Esfe [4] designed an ANN to model the $k_{nf}$ of ethylene glycol– $H_2O$ / $TiO_2$ nanofluids. He showed that ANNs are very powerful in modeling the $k_{nf}$ of nanofluids. Esfe et al. [5] estimated the $k_{nf}$ of SWCNT–$Al_2O_3$/ ethylene glycol nanofluid using correlation and ANN methods. Esfe et al. [6] predicted the $k_{nf}$ of MWCNT/ Ethylene Glycol nanofluid using ANN. Alrashed et al. [7] investigated the properties of carbon-based data using experimental and ANN methods. Mohamed and Habashy [8] predicted the $k_{nf}$ modeling of Propylene Glycol-based nanofluids using the ANN method. Their results demonstrate the ability of the ANN model in the nanofluid field. Aghayari et al. [9] studied the electrical conductivity of CuO/Glycerol nanofluids with the ANN method. Karimipour et al. [10] obtained a correlation for estimating the $k_{nf}$ and viscosity of CuO/liquid paraffin nanofluid using ANN. Eshgarf et al. [11] predicted the rheological behavior of MWCNTs–$SiO_2$/ Ethylene Glycol–$H_2O$ nanofluid using ANNs. Esfe et al. [12] modeled the $k_{nf}$ of DWCNT–$SiO_2$/Ethylene Glycol nanofluid using ANNs. By comparing the experimental data for $k_{nf}$ with ANN data, they showed the high capacity and accuracy of ANN in $k_{nf}$ predicting. Zendehboudi and Saidur [13] modeled the effective $k_{nf}$ of 26 nanofluids using the MLP-ANN approach. Amani et al. [14] predicted the properties of the aqueous solution of $TiO_2$/CMC- $H_2O$ nanofluid using ANN. Rahman and Zhang [15] studied the heat transfer coefficient of the thermo-acoustic heat exchanger by ANNs. Longo et al. [16] modeled the viscosity of the $H_2O$ / KCOOH mixture by the ANNs. Zhi et al. [17] studied the viscosity of refrigerants by using the ANNs. Gülüm et al. [18] studied the viscosity of 6 pure refrigerants by the ANNs and regression models. Bahrami et al. [19] developed an ANN method. Ahmadi et al. [20] studied the viscosity of Ag/$H_2O$ nanofluids using ANNs. Mohamadian et al. [21] studied the viscosity of Ag/ $H_2O$ nanofluids. using the ANN. Also, Cong et al. [22,23] investigated different aspect of nanofluids in different situations. Another aspects of nanofluids using ANN were done by Ruhani et al. [24] from different aspects.

In this study, the $k_{nf}$ of ZnO -$TiO_2$ (50 %–50 %)/ Ethylene Glycol hybrid nanofluid using ANNs was predicted. A surface fitting method was applied to predict the $k_{nf}$ of hybrid nanofluid. Finally, the correlation coefficients, performances, and MAEs for both methods have been presented and compared. The ANN is a simple method that prevents the extraction of experimental data and reduces cost by predicting the behavior of nanofluids. So using this simple method to predict the behavior of the nanofluid is the nobility of this work.

A simple method to predict the $k_{nf}$ of ZnO -$TiO_2$ (50 %–50 %)/ Ethylene Glycol hybrid nanofluid was used in this work. This method is useful for a small number of data points with a simple behavior. The model of this nanofluid has a simple behavior, and other machine learning methods such as ANFIS/Fuzzy logic may increase the uncertainty of the artificial model and are suitable for complicated models. For instance, in the fuzzy logic method selecting suitable membership functions and the number of them should be selected appropriately to obtain acceptable results. In addition, in this paper, an inner iteration method was used, which runs the program several times, and for each neuron number, the average value of running the program is shown. This inner iteration increases the reliability of results. In the next papers, we plan to use and compare the results of this method with other machine learning methods in predicting the $k_{nf}$ of nanofluid. None of them is focused on the $k_{nf}$ of ZnO –$TiO_2$ / Ethylene Glycol hybrid nanofluid in all the mentioned researches. As this nanofluid is used in many engineering applications, it is important to design a specific ANN for this nanofluid and predict the behavior rapidly. This study aims to design a suitable ANN to predict the behavior of nanofluids. By using ANNs, the lab cost decreases, but the required time to obtain $k_{nf}$ is decreased.

## 2. Experimental results

A two-stage method was used to produce the nanofluid. To produce nanofluids in a different $\varphi$, the mass values needed to produce arbitrary $\varphi$ are calculated. The mixture was sub-

jected to ultrasonic waves for 4, 8, and 12 h. The nanofluid had good stability, and no sedimentation was observed. Tables 1 and 2 show the properties of the ZnO and $TiO_2$ nanoparticles. Table 3 also shows the chemical properties of ethylene glycol [25].

Fig. 1and Fig. 2 show the variation of the $k_{nf}$ versus $\varphi$ and temperature (T) [25]. At T = 25 °C, at $\varphi = 0.001$, the $k_{nf}$

**Table 1** The properties of the ZnO[25].

| ***Properties*** | |
|---|---|
| *Molecular formula* | *ZnO* |
| *Nanoparticle shape* | *Spherical* |
| *Size* | $35-45\ nm$ |
| *Purity* | 99% |
| *Appearance* | *White* |
| *Density* | $5.606 g/cm^3$ |
| *Specific Area* | $20-60\ m^2/g$ |

**Table 2** The properties of the $TiO_2$ [25].

| ***Properties*** | |
|---|---|
| *Molecular formula* | $TiO_2$ |
| *Nanoparticle shape* | *Spherical* |
| *Size* | $30\ nm$ |
| *Purity* | 99% |
| *Appearance* | *White* |
| *Density* | $0.46\ g/cm^3$ |
| *Specific Area* | $10-45\ m^2/g$ |

**Table 3** Properties of the ethylene glycol [25].

| ***Properties*** | ***Value*** |
|---|---|
| *Combustion temperature °C* | 410 |
| *Saturation concentration* $(g/m^3)$ | 15 |
| *Melting point °C* | −13 |
| *Molar mass* $(g/mol)$ | 62.07 |
| *Density* $(g/cm^3)$ | 1.114 |
| *pH value* | 6.5 – 7 |
| *Boiling point °C* | 197.6 |
| *Steam pressure °C* | 410 |

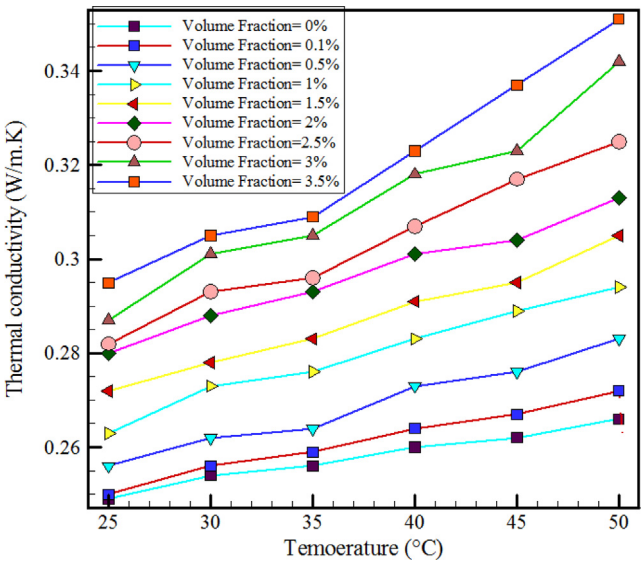


**Fig. 1** Variation of the $k_{nf}$ versus temperature at different $\varphi$ [25].

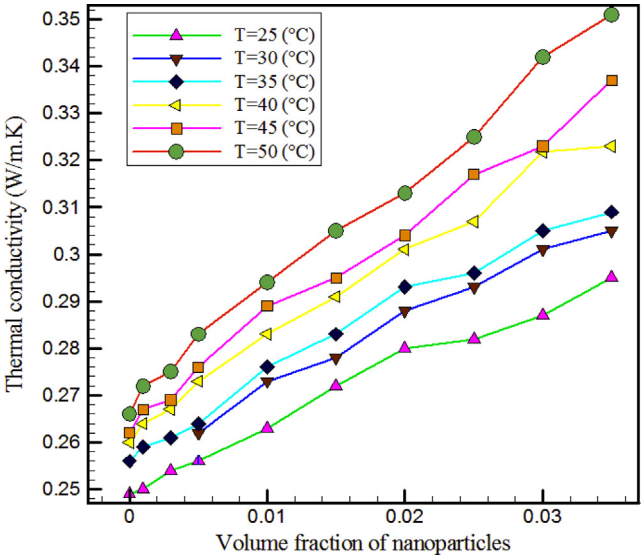


**Fig. 2** Variation of the $k_{nf}$ versus $\varphi$ at different temperatures [25].

increased by 0.4 % compared to the thermal conductivity of base $k_{bf}$ at the same temperature. At $\varphi = 0.003$, the $k_{nf}$ increases by 2 %, and at $\varphi = 0.005$, the $k_{nf}$ increases by 2.8 % relative to the base fluid. At $\varphi = 0.01$, the $k_{nf}$ increased by 5.6 %, and at $\varphi = 0.015$, the $k_{nf}$ increased by 9.2 % relative to the $k_{bf}$ at T = 25 °C. Similarly, at $\varphi = 0.02$ and $\varphi = 0.025$, 0.03 and 0.035, the $k_{nf}$ increased by 12.45, 13.3 and 15.3 and 18.5 %, respectively. According to the data presented at T = 25 °C, we find that by increasing $\varphi$ from 0.001 to 0.035, the $k_{nf}$ increases from 0.4 to 18.5 %, and the highest $k_{nf}$ is increased. There is the highest $k_{nf}$ in the highest $\varphi$. At $\varphi = 0.015$, we had the highest slope increase in $k_{nf}$ (3.4 %). At T = 30 °C, the $k_{nf}$ increased from 0.8 to 20.1 % relative to the base fluid by increasing the $\varphi$ from 0.001 to 0.035. The highest $k_{nf}$ is related to the highest $\varphi$ at this temperature. The obtained data also show that at T = 30 °C and $\varphi = 0.035$, the $k_{nf}$ increased by about 22.4 % when the base fluid was at T = 25 °C. Also, at T = 35 °C, the $k_{nf}$ increases by 1.2 % with an increase of $\varphi = 0.001$ at the same temperature. The higher $\varphi$ at a constant temperature, the higher the $k_{nf}$ increases. The highest percentage of increase in $k_{nf}$ was $\varphi = 0.035$, in which the $k_{nf}$ increased by about 20.7 % relative to the $k_{bf}$ at T = 35 °C. At T = 40 °C, the $k_{nf}$ increased by 1.5 % at t $\varphi = 0.001$, and by increasing the $\varphi$ to 0.035, the $k_{nf}$ increased to 24.2 % relative to the base fluid at the same temperature. The data also show that if the base fluid temperature increases from T = 25 °C to T = 40 °C, and at $\varphi = 0.035$, the $k_{nf}$

**Table 4** The sorted performances.

| *Neuron Number* | *All* | *Train* | *Validation* | *Test* |
|---|---|---|---|---|
| 7 | 2.2E-06 | 1.33E-06 | 2.1E-06 | 6.38E-06 |
| 9 | 2.25E-06 | 1.25E-06 | 2.09E-06 | 7.25E-06 |
| 8 | 2.31E-06 | 1.62E-06 | 1.23E-06 | 7.79E-06 |
| 10 | 2.81E-06 | 9.34E-07 | 3.41E-06 | 1.08E-05 |
| 6 | 2.85E-06 | 1.66E-06 | 3.78E-06 | 5.91E-06 |
| 12 | 2.9E-06 | 1.1E-06 | 3.57E-06 | 1.02E-05 |
| 13 | 3.05E-06 | 1.61E-06 | 2.8E-06 | 1.05E-05 |
| 11 | 3.78E-06 | 2.43E-06 | 3.13E-06 | 1.13E-05 |
| 15 | 3.89E-06 | 1.85E-06 | 3.9E-06 | 1.37E-05 |
| 16 | 4.38E-06 | 2.36E-06 | 3.13E-06 | 1.69E-05 |
| 14 | 4.74E-06 | 2.2E-06 | 6.12E-06 | 1.36E-05 |
| 18 | 5.05E-06 | 1.41E-06 | 6.11E-06 | 2.09E-05 |
| 21 | 5.93E-06 | 1.41E-06 | 6.26E-06 | 2.83E-05 |
| 20 | 6.44E-06 | 2.09E-06 | 6.77E-06 | 2.76E-05 |
| 22 | 6.62E-06 | 1.73E-06 | 5.76E-06 | 3.37E-05 |
| 19 | 7.31E-06 | 3.94E-06 | 7.52E-06 | 2.26E-05 |
| 25 | 7.6E-06 | 1.61E-06 | 1.06E-05 | 3.08E-05 |
| 17 | 7.94E-06 | 1.83E-06 | 1.24E-05 | 2.82E-05 |
| 24 | 8.81E-06 | 3.03E-06 | 1.27E-05 | 2.81E-05 |
| 23 | 9.14E-06 | 3.01E-06 | 1.17E-05 | 3.36E-05 |
| 27 | 1.03E-05 | 1.92E-06 | 1.56E-05 | 4.09E-05 |
| 28 | 1.09E-05 | 1.11E-06 | 1.83E-05 | 4.38E-05 |
| 26 | 1.15E-05 | 3.06E-06 | 1.1E-05 | 5.6E-05 |
| 30 | 1.31E-05 | 1.49E-06 | 1.51E-05 | 6.89E-05 |
| 33 | 1.72E-05 | 1.09E-06 | 2.41E-05 | 8.44E-05 |
| 34 | 1.86E-05 | 8.77E-07 | 2.48E-05 | 9.64E-05 |
| 35 | 2.09E-05 | 1.33E-06 | 2.81E-05 | 0.000106 |
| 31 | 2.28E-05 | 6.53E-06 | 2.61E-05 | 9.77E-05 |
| 32 | 2.37E-05 | 1.28E-06 | 3.59E-05 | 0.000111 |
| 29 | 2.55E-05 | 3.6E-06 | 3.32E-05 | 0.000121 |
| 39 | 3.07E-05 | 6.37E-07 | 4.6E-05 | 0.000151 |
| 36 | 3.24E-05 | 5.19E-06 | 3.62E-05 | 0.000164 |
| 38 | 4.31E-05 | 4.67E-06 | 5.92E-05 | 0.000204 |
| 37 | 4.48E-05 | 3.14E-06 | 4.88E-05 | 0.000254 |
| 40 | 4.91E-05 | 3.72E-06 | 5.22E-05 | 0.00028 |
| 43 | 4.92E-05 | 1.53E-06 | 7.94E-05 | 0.000226 |
| 42 | 5.07E-05 | 4.63E-06 | 6.15E-05 | 0.000265 |
| 41 | 5.31E-05 | 3.9E-06 | 9.14E-05 | 0.000216 |
| 44 | 5.39E-05 | 5.34E-07 | 6.72E-05 | 0.000303 |

**Table 5** The correlation coefficients for each neuron number.

| *Neuron Number* | R | R1 | R2 | *R*3 |
|---|---|---|---|---|
| 7 | 0.996408 | 0.998003 | 0.992682 | 0.991524 |
| 9 | 0.996342 | 0.998112 | 0.993321 | 0.993741 |
| 8 | 0.996258 | 0.997457 | 0.995205 | 0.988033 |
| 10 | 0.995372 | 0.998445 | 0.990884 | 0.98796 |
| 6 | 0.99565 | 0.997548 | 0.995634 | 0.994005 |
| 12 | 0.995378 | 0.998478 | 0.988871 | 0.986751 |
| 13 | 0.994914 | 0.997431 | 0.991467 | 0.983863 |
| 11 | 0.994042 | 0.996348 | 0.99051 | 0.985528 |
| 15 | 0.993712 | 0.997173 | 0.989468 | 0.981872 |
| 16 | 0.992675 | 0.9963 | 0.990286 | 0.977253 |
| 14 | 0.992254 | 0.996272 | 0.987153 | 0.979813 |
| 18 | 0.991768 | 0.997862 | 0.974766 | 0.970645 |
| 21 | 0.990939 | 0.997799 | 0.984474 | 0.97453 |
| 20 | 0.98983 | 0.996561 | 0.98447 | 0.973256 |
| 22 | 0.989483 | 0.997365 | 0.983885 | 0.957353 |
| 19 | 0.988108 | 0.994202 | 0.962737 | 0.975589 |
| 25 | 0.987647 | 0.997675 | 0.973996 | 0.9556 |
| 17 | 0.987228 | 0.997373 | 0.97737 | 0.968359 |
| 24 | 0.986141 | 0.995734 | 0.972567 | 0.955081 |
| 23 | 0.985377 | 0.995455 | 0.962215 | 0.966306 |
| 27 | 0.982889 | 0.997219 | 0.944049 | 0.946039 |
| 28 | 0.983129 | 0.998293 | 0.945474 | 0.955797 |
| 26 | 0.981434 | 0.995218 | 0.973833 | 0.938514 |
| 30 | 0.979061 | 0.997615 | 0.967882 | 0.916838 |
| 33 | 0.972656 | 0.998428 | 0.918362 | 0.923039 |
| 34 | 0.97146 | 0.998673 | 0.93972 | 0.884858 |
| 35 | 0.967486 | 0.997972 | 0.886178 | 0.844234 |
| 31 | 0.968292 | 0.990142 | 0.951656 | 0.867087 |
| 32 | 0.964415 | 0.998207 | 0.891629 | 0.891489 |
| 29 | 0.962931 | 0.995003 | 0.919799 | 0.869147 |
| 39 | 0.951447 | 0.998996 | 0.90129 | 0.856993 |
| 36 | 0.951317 | 0.991509 | 0.902888 | 0.861279 |
| 38 | 0.933728 | 0.991175 | 0.854761 | 0.863626 |
| 37 | 0.935564 | 0.994833 | 0.861104 | 0.827856 |
| 40 | 0.930498 | 0.993784 | 0.882899 | 0.746966 |
| 43 | 0.932363 | 0.997679 | 0.83899 | 0.820589 |
| 42 | 0.936206 | 0.994012 | 0.881158 | 0.869328 |
| 41 | 0.921527 | 0.994123 | 0.81245 | 0.822816 |
| 44 | 0.929825 | 0.999186 | 0.881939 | 0.748685 |

increases by 29.72 %. At T = 45 °C and T = 50 °C, the $k_{nf}$ also increases with increasing $\varphi$. Also, increasing the temperature in each $\varphi$ increases the $k_{nf}$. At T = 50 °C, the $k_{nf}$ increased by about 40.1 % over ethylene glycol at T = 25 °C, indicating a significant contribution of increasing temperature and $\varphi$ to increase the $k_{nf}$. The higher the $\varphi$, the more particles are joined together and form larger clusters, which increases the $k_{nf}$ due to the faster movement of heat through the paths of these clusters. Increasing the temperature also increases the Brownian motion and more collisions of the fluid molecules and the molecules of the fluid and the particles and the molecules of each other, increasing the $k_{nf}$. With increasing temperature, the mixing in the layers increases. By raising the temperature, the effects of the surfactant disappear, resulting in a decrease in the $k_{nf}$ [25].

Considering Figs. 1 and 2, it can be seen that $k_{nf}$ has a direct relationship to temperature. In addition, as the $\varphi$ increases, the $k_{nf}$ increases. Therefore, the best $k_{nf}$ occurs by higher temperature and higher $\varphi$. [25].

## 3. ANN method

### 3.1. Fundamental of ANN

ANNs are intelligent model-free dynamic systems based on experimental data that do not require receivers and process the knowledge or law behind the data into the network structure by processing the experimental data. The process of data is presented in Eq. (1),

$$T_i = f\left(\sum_{j=1}^{N} w_{ij}x_j + b_i\right) \tag{1}$$

here, $T_i$, f, n, $w_{ij}$, $x_j$, and $b_i$ represent the output, the activation function, the number of experimental data, the weight matrix, the input, and the bias, respectively. In the current work, the number of the data point is 60 and 70 percent of data is considered for the train, 15 % for validation and the rest of the data is for the test. The train data generates the weight and biases of the matrix, the validation data adjust and modify the

weights and biases during the learning process. Finally, the test data is used to determine the performance of the network. The ANN performance is considered as Mean Square Error (MSE) which is defined in Eq. (2),

$$MSE = \frac{1}{n}\sum_{i=1}^{n}\sqrt{\left(T_i - \widehat{T}_i\right)^2} \tag{2}$$

here, $n$ represent the number of data points (60), $T_k$ represent the experimental target and $\widehat{T}_i$ represent the output of ANN. The learning algorithm is Levenberg Marquardt or the Damped Least square method. In this study, the activation function for the last layer is the pure line and for other layers is tan $sig(x)$. The tangent sigmoid function is shown in Eq.3,

$$\tan sig(x) = \frac{2}{1+e^{-2x}} - 1 \tag{3}$$

In designing the ANN, it is important to avoid overfitting. In an ANN with overfitting, the network can predict data points in a very limited range, or it only can predict the train data. But it fails in the test data points which are introduced to the ANN for the first time. The overtrained network can't follow the trend of data. We used the designed ANN outside of this range and compared the results of ANN to them. But as we had few data points outside of the mentioned ranges, we didn't discuss these extra points, and these few points are only used to be ensuring that the designed ANN has not any overfitting and can follow the trend of data.

In the current study, as the ANN should predict the $k_{nf}$, only one neuron should be in the output layer. But in the hidden layer, the number of neurons can be different. The neuron numbers have an important effect on the predicted results. The bounds of neuron numbers are calculated considering Eq. (4),

$$Bounds: \begin{cases} LB = 2(n_i + n_o) \\ UB = (N*(n_i+n_o) - n_o)/(n_i + n_o + 1) \end{cases} \tag{4}$$

In the above equation, $n_i$ represent the number of input variables (2) and $n_o$ represent the number of outputs parameters (1), and $N$ represent the number of data samples. The lower and upper bounds of this study are 6 and 44, respectively. As the weights and biases during each simulation are different, the ANN may have different results for a specific neuron number. An internal loop is designed to improve the reliability of performance for a specific neuron number. This loop simulates the network several times (in this study, it simulates for 15 times), and the mean statistical outputs are considered the result of that neuron number. The algorithm to determine the best neuron number in the hidden layer is presented as follows:

### 3.2. The best neuron number algorithm

As mentioned before, in this study, $\varphi$ and temperature considered as input parameters, $n_o$ the number of outputs ($k_{nf}$) $n_s$ is considered as the number of experimental data (60) from Ref. [25]. Undeniably, $k_{nf}$ is affected by other factors. But, these are the most important factor, and $k_{nf}$ is affected more by these two items ($k_{nf}$ and $\varphi$). In Table 4, the performances are sorted and presented for train validation and test data points.

In Table 4, the performances for train, validation, test, and all outputs have been presented. Results show that the best ANN has 7 neuron numbers in the hidden layer and the best performance represents the ANN with 7 neurons. Although the results of some other neuron numbers are similar to this ANN, the criteria of selecting the best ANN is based on the best performances for tests and overall outputs. The ANN with 7 neurons has the best these two performances (test and overall). The correlation coefficients of each neuron number have been presented In Table 5. The correlation coefficient can be calculated using Eq. (5),

$$\rho_{U,V} = \frac{E[(U-\mu_U)(V-\mu_V)]}{\sigma_U \sigma_Y} \tag{5}$$

here, $U$, $V$ represent the Targets and predicted values respectively, $\mu_U$ and $\mu_V$ represent the mean value of $U$ and $V$. The standard deviations $U, V$ represent $\sigma_U, \sigma_V$ respectively and $\rho$

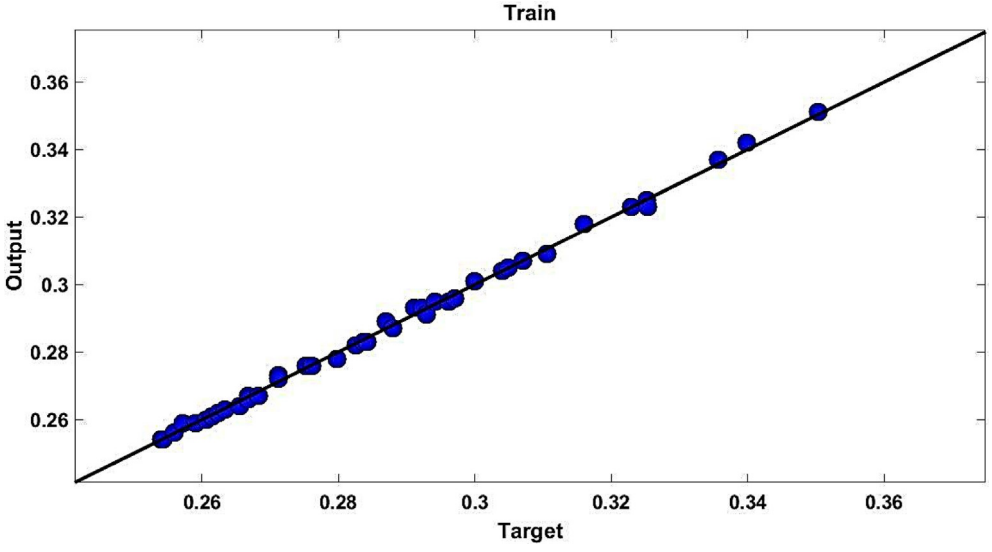


**Fig. 3** Train data outputs of ANN.

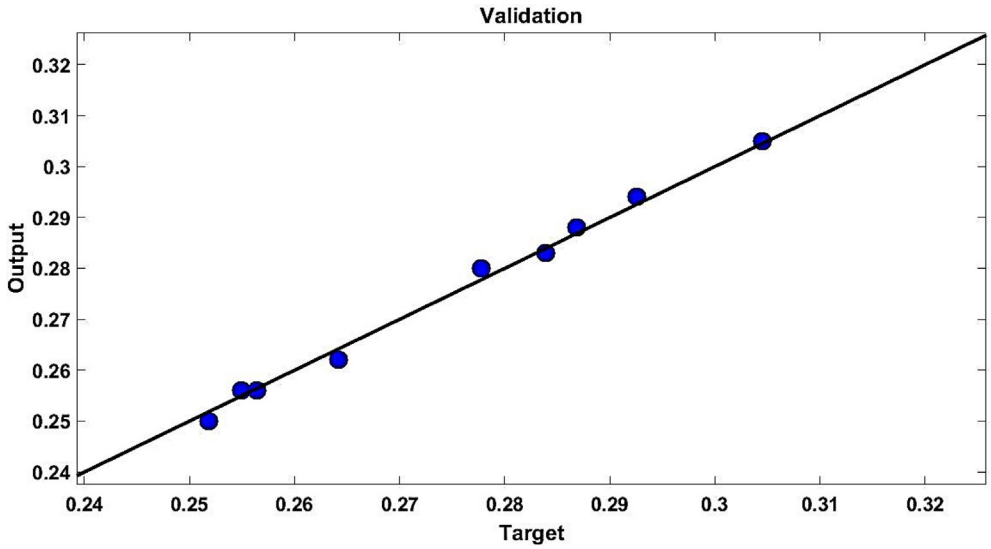


**Fig. 4** Validation data outputs of ANN.

represent the correlation coefficient between the experimental and predicted values. In Table 5, $R, R1, R2, R3$ represent all data, train data, validation data, and test data correlation coefficients.

The represented results in Tables 4 and 5 show that the ANN with 7 neuron numbers in the hidden layer has the best performance and has the best correlation coefficient. Considering Tables 4 and 5, different neuron numbers are applied, and based on the results, the optimum neuron number is 7. The neuron numbers in Table 4 are sorted based on the overall performance. The results show that the best number of neurons is 7, although some neuron numbers have acceptable performance. In addition, the ANN results of Table 4 are the mean value of several times of running the program for each neuron number to increase the reliability of results (inner iteration number is 20). Therefore, these results for each neuron number are obtained by running the program after 20 times. In this study, $\varphi$ and temperature are considered inputs, and knf is considered a target. In this study, $\varphi$ and temperature is input parameters and $k_{nf}$ is used as a target parameter. The train, validation, and test outputs are presented in Figs. 3 to 6. In train data, the MSE is 1.3324e-06, and MAE is 0.0024. In the validation data, the MSE is 2.0966e-06 and MAE is 0.0023. In test data, the MSE is 6.3805e-06 and MAE is 0.0039. In all data points, MSE is 2.2043e-06 and MAE is 0.0039.

## 4. Fitting method

In a different method, a fitting method is used to predict the $k_{nf}$ of this hybrid nanofluid. A third-order function is used for $\varphi$ and a first-order function is used for the temperature to predict $k_{nf}$. The higher-order function for the temperature doesn't improve the performance of the fitting method. Each

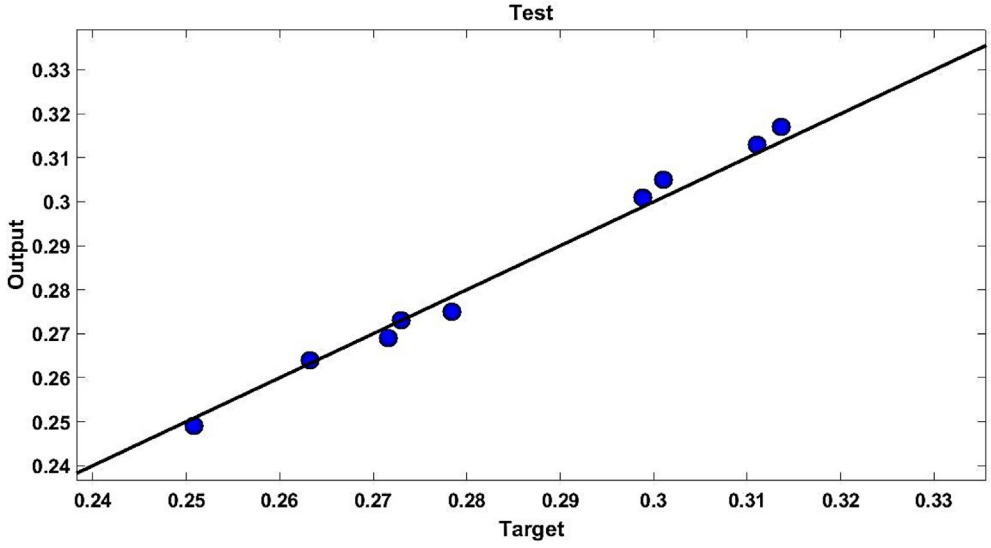


**Fig. 5** Test data outputs of ANN.

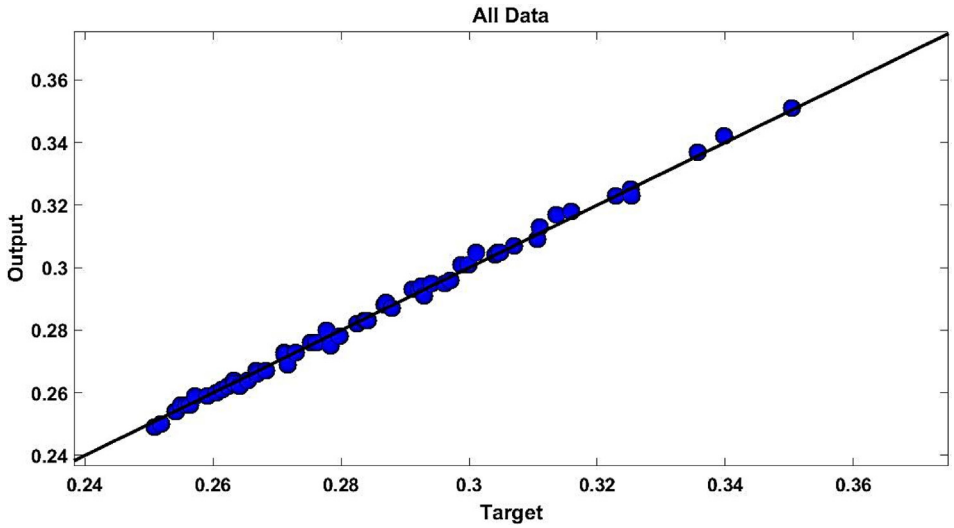


**Fig. 6** All data outputs of ANN.

**Table 6** The values of fitted surface coefficients.

| *P*00 | *P*10 | *P*01 | *P*20 | *P*11 | *P*30 | *P*21 |
|---|---|---|---|---|---|---|
| 0.229025 | 0.013641 | 0.000776 | −0.004636 | 0.000259 | 0.000390 | 0.000044 |

dataset has its specifications, and the fitted functions cannot be extended to all data set. For this study, we first tried higher orders for the fitting function, but there was not a significant difference between these orders. In addition, higher orders may fluctuate outside the specified boundaries and may not be used outside these boundaries. In other words, lower orders are better, especially when we want to consider extrapolation and predict the behavior of nanofluids out of these ranges. The fitted function is presented in Eq. (6),

$$Fit\_function(x,y) = P00 + P10*x + P01*y + P20*x^2 + P11*x*y + P30*x^3 + P21*x^2*y \quad (6)$$

In the presented function, x and y represent $\varphi$ and the temperature, respectively. The values of fitted surface coefficients are reported in Table 6 and represented in Fig. 7.

This surface depicts a better overview of the behavior of nanofluids. It can be seen that $k_{nf}$ has a direct relationship to

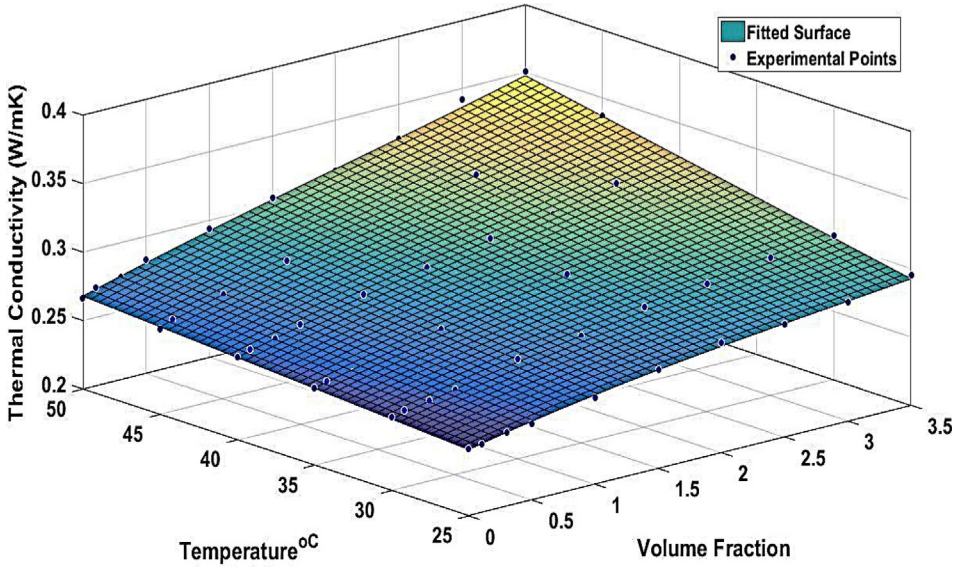


**Fig. 7** The fitted surface on the experimental data points.

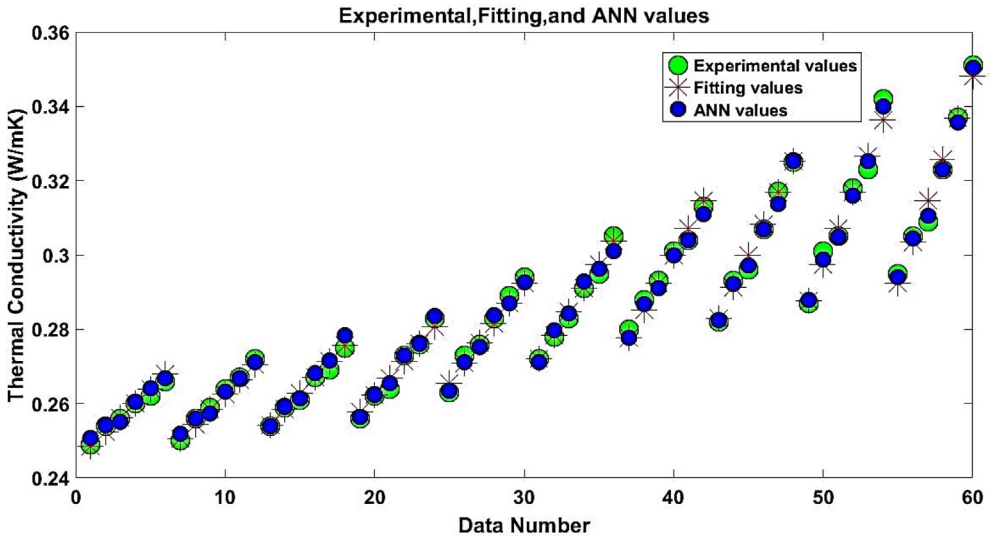


**Fig. 8** The experimental, fitting, and ANN values.

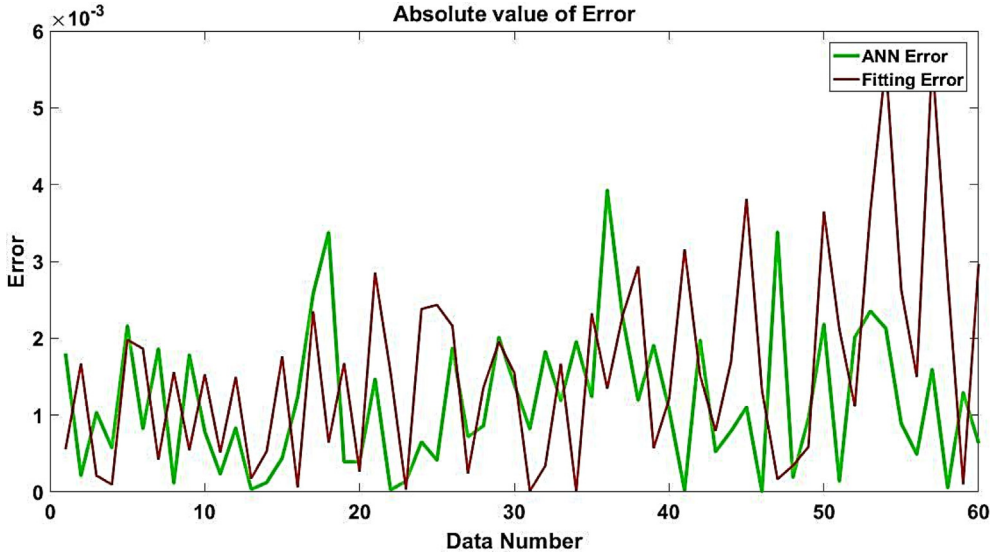


**Fig. 9** The value of AE for ANN and fitting method.

temperature and $\varphi$. The maximum $k_{nf}$ occurs in the highest values of temperature and $\varphi$. In Fig. 8, the experimental, fitting values, and ANN outputs are presented. It is found that both the ANN and fitting method have acceptable accuracy in predicting the $k_{nf}$ based on the temperature and $\varphi$. It can be seen that ANN and fitting methods are near the experimental data points, and both these methods are accurate enough to predict $k_{nf}$.

In Fig. 9, the value of absolute error (AE) for both the ANN and fitting method is presented. We assumed that the experimental data are our reference values; however, the error of extracting the experimental data may be more than 0.003, and we tried to predict these reference values.

The difference between the experimental data points and the predicted values is defined as an error. The dimension of error is like $k_{nf}\,(W/mK)$. Considering Fig. 9, the fitting method has bigger AE values compared to the ANN method. Although the scale of errors is very small, the ANN, with less amount of AE, can predict the behavior of this nanofluid better than the bonding method. In other words, the output ($k_{nf}$) has a direct relationship to the both temperature and $\varphi$. So, as the magnitudes of these values are increasing, the effect of them on the output also increases and the error also increases. In Table 7, some statistical data including MAE, MSE, and correlation coefficient for ANN and fitting methods are pre-

**Table 7** Statistical parameters.

| | ANN | Fitting |
|---|---|---|
| *MAE* | 0.0039 | 0.0056 |
| *MSE* | $2.20E-06$ | $4.08E-06$ |
| *Correlation coefficient* | 0.996408 | 0.996217 |

sented. The results of Table 7 show that the ANN method has better values in all three presented measures.

## 5. Conclusion

In this study, we predicted the $k_{nf}$ of a hybrid nanofluid using ANNs. The nanofluid was prepared by dispersing ZnO -$TiO_2$ nanoparticles in ethylene glycol. In addition, $\varphi$ has a direct effect on $k_{nf}$. In other words, to improve $k_{nf}$, temperature and $\varphi$ should be increased. Regarding the ANN outputs, it can be understood that the ANN method has a better ability in predicting the behavior of nanofluid compared to the fitting method. The strength of this method is its simplicity and accuracy in predicting data points. But its performance outside the trained range should be evaluated in some researches. Like many ANNs, these networks are valid inside the trained intervals, and the accuracy and performances cannot be guaranteed outside these ranges. The ANN method not only showed better performance but also reached a better MAE and correlation coefficient. Finally, as reported in this article, the output variables ($k_{nf}$ values) can be continuous instead of discretized. In continuous variables, the Machine Learning (ML) algorithms usually implemented are ML regressions instead of conventional ML. Therefore, using sparse and non-sparse ML regressions such as ANN regression can be easily implemented, with continuous outputs predictions. All of them can be implemented with accessible user-interface libraries in Phyton, MatLab, etc.

## Declaration of Competing Interest

The authors declare that they have no known competing financial interests or personal relationships that could have appeared to influence the work reported in this paper.

## References


[1] B. Ruhani et al., Statistical modeling and investigation of thermal characteristics of a new nanofluid containing cerium oxide powde, Heliyon 8 (11) (2022) 11373.

[2] W. He et al, Using of artificial neural networks (ANNs) to predict the thermal conductivity of zinc oxide–silver (50%–50%)/water hybrid Newtonian nanofluid, Int Commun Heat Mass Transf. 116 (2020) 104645.

[3] S.K. Mechiri, V. Vasu, S. Babu, Thermal conductivity of Cu-Zn Hybrid Newtonian Nanofluids: Experimental Data and Modeling using Neural Network, Procedia Eng. 127 (2015) 561–567.

[4] M.H. Esfe, Designing an ANN using radial basis function (RBF-ANN) to model thermal conductivity of ethylene glycol–water-based $TiO_2$ nanofluids, J. Therm. Anal. Calorim. 127 (2017) 2125.

[5] M.H. Esfe, M. Rejvani, R. Karimpour, A.A. Abbasian Arani, Estimation of thermal conductivity of ethylene glycol-based nanofluid with hybrid suspensions of SWCNT–$Al_2O_3$ nanoparticles by correlation and ANN methods using experimental data, J. Therm. Anal. Calorim. 128 (2017) 1359.

[6] M. Hemmat Esfe, S. Wongwises, M. Rejvani, Prediction of thermal conductivity of carbon nanotube-EG nanofluid using experimental data by ANN, Curr. Nanosci., 13(3) 2017, 324-329 (6).

[7] A.A. Alrashed, M.S. Gharibdousti, M. Goodarzi, L.R. de Oliveira, M.R. Safaei, E.P. Bandarra Filho, Effects on thermophysical properties of carbon based nanofluids: Experimental data, modeling using regression, ANFIS and ANN, Int. J. Heat Mass Transf. 125 (2018) 920–932.

[8] R. Mohamed, D. Habashy, Thermal conductivity modeling of propylene glycol - based nanofluid using ANN, J. Adv. Phys. 14 (1) (2018) 5281–5291.

[9] R. Aghayari, H. Maddah, M.H. Ahmadi, W.-M. Yan, N. Ghasemi, Measurement and ANN modeling of electrical conductivity of CuO/Glycerol nanofluids at various thermal and concentration conditions, Energies 11 (2018) 1190.

[10] A. Karimipour, S. Ghasemi, M.H.K. Darvanjooghi, A. Abdollahi, A new correlation for estimating the thermal conductivity and dynamic viscosity of CuO/liquid paraffin nanofluid using neural network method, Int. Commun. Heat Mass Transfer 92 (2018) 90–99.

[11] N.S. Eshgarf, Mohammad Hemmat Esfe, Farhad Izadi, Masoud Afrand, Prediction of rheological behavior of MWCNTs–$SiO_2$/EG–water non-Newtonian hybrid nanofluid by designing new correlations and optimal ANNs, J. Therm. Anal. Calorim. 132 (2018) 1029.

[12] M. Hemmat Esfe, A.A. Abbasian Arani, R. Shafiei Badi, M. Rejvani, ANN modeling, cost performance and sensitivity analyzing of thermal conductivity of DWCNT–$SiO_2$/EG hybrid nanofluid for higher heat transfer, J. Therm. Anal. Calorim. 131 (2018) 2381.

[13] A. Zendehboudi, R. Saidur, A reliable model to estimate the effective thermal conductivity of nanofluids, Heat Mass Transf. 55 (2019) 397.

[14] M. Amani, P. Amani, M. Bahiraei, S. Wongwises, Prediction of hydrothermal behavior of a non-Newtonian nanofluid in a square channel by modeling of thermophysical properties using neural network, J. Therm. Anal. Calorim. 135 (2019) 901.

[15] A.A. Rahman, X. Zhang, Prediction of oscillatory heat transfer coefficient for a thermoacoustic heat exchanger through ANN technique, Int. J. Heat Mass Transf. 124 (2018) 1088–1096.

[16] A. Giovanni, Longo, Ludovico Ortombina, Mauro Zigliotto, Application of ANN for modelling $H_2O$/KCOOH (potassium formate) dynamic viscosity, Int. J. Refrig 86 (2018) 435–440.

[17] L.-H. Zhi, H.u. Peng, L.-X. Chen, G. Zhao, Viscosity prediction for six pure refrigerants using different ANNs, Int. J. Refrig 88 (2018) 432–440.

[18] M. Gülüm, F.K. Onay, A. Bilgin, Comparison of viscosity prediction capabilities of regression models and ANNs, Energy 161 (2018) 361–369.

[19] M. Bahrami, M. Akbari, S.A. Bagherzadeh, A. Karimipour, M. Afrand, M. Goodarzi, Develop 24 dissimilar ANNs by suitable architectures & Training algorithms via sensitivity analysis to better statistical presentation: Measure MSEs between targets & ANN for Fe–CuO/EG–Water nanofluid, Physica A 519 (2019) 159–168.

[20] M.H. Ahmadi, B. Mohseni-Gharyehsafa, M. Farzaneh-Gord, R.D. Jilte, R. Kumar, K.W. Chau, Applicability of connectionist methods to predict dynamic viscosity of silver/water nanofluid by using ANN-MLP, MARS and MPR algorithms, Eng. Applications Computational Fluid Mech. 13 (1) (2019) 220–228.

[21] F. Mohamadian, L. Eftekhar, Y.H. Bardineh, Applying GMDH artificial neural network to predict dynamic viscosity of an antimicrobial nanofluid, 5(4) (2018) 217.
[22] Y. Wang, C. Qi, Z. Ding, J. Tu, R. Zhao, Numerical simulation of flow and heat transfer characteristics of nanofluids in built-in porous twisted tape tube, Powder Technol. 392 (2021) 570–586, https://doi.org/10.1016/j.powtec.2021.07.066.
[23] F. Fan, C. Qi, J. Tu, Z. Ding, Effects of variable magnetic field on particle fouling properties of magnetic nanofluids in a novel thermal exchanger system, Int. J. Therm. Sci. 175 (2022), https://doi.org/10.1016/j.ijthermalsci.2022.107463 107463.
[24] B. Ruhani et al, Statistical investigation for developing a new model for rheological behavior of Silica–ethylene glycol/Water hybrid Newtonian nanofluid using experimental data, Phys. A: Stat. Mech. Appl. 525 (2019) 616–627.
[25] D. Toghraie, V.A. Chaharsoghi, M. Afrand, Measurement of thermal conductivity of ZnO–$TiO_2$/EG hybrid nanofluid, J. Therm. Anal. Calorim. 125 (2016) 527–535, https://doi.org/10.1007/s10973-016-5436-4.